Talanta 88 (2012) 403–407

Contents lists available at SciVerse ScienceDirect

Talanta

journal homepage: www.elsevier.com/locate/talanta

Thiolated DAB dendrimers and CdSe quantum dots nanocomposites for Cd(II) or Pb(II) sensing

M. Algarra[a], B.B. Campos[b], B. Alonso[c], M.S. Miranda[a], Á.M. Martínez[c], C.M. Casado[c], J.C.G. Esteves da Silva[b,*]

[a] Centro de Geologia, Departamento de Geociências, Ambiente e Ordenamento do Território do Porto, Faculdade de Ciências, Universidade do Porto, Rua do Campo Alegre 687, 4169-007 Porto, Portugal
[b] Centro de Investigação em Química, Departamento de Química e Bioquímica, Faculdade de Ciências, Universidade do Porto, Porto, Portugal
[c] Departamento de Química Inorgánica, Universidad Autónoma de Madrid, Cantoblanco 28049, Madrid, Spain

ARTICLE INFO

Article history:
Received 26 July 2011
Received in revised form 25 October 2011
Accepted 1 November 2011
Available online 6 November 2011

Keywords:
DAB dendrimer
Nanocomposite sensor
CdSe quantum dots
Thiolated DAB dendrimer
Cd(II)
Pb(II)

ABSTRACT

Four different generation of thiol-DAB dendrimers were synthesized, S-DAB-G_x (x = 1, 2, 3 and 5), and coupled with CdSe quantum dots, to obtain fluorescent nanocomposites as metal ions sensing. Cd(II) and Pb(II) showed the higher enhancement and quenching effects respectively towards the fluorescence of S-DAB-G_5-CdSe nanocomposite. The fluorescence enhancement provoked by Cd(II) can be linearized using a Henderson–Hasselbalch type equation and the quenching provoked by Pb(II) can be linearized by a Stern–Volmer equation. The sensor responds to Cd(II) ion in the 0.05–0.7 μM concentration range and to Pb(II) ion in the 0.01–0.15 mM concentration range with a LOD of 0.06 mM. The sensor has selectivity limitations but its dendrimer configuration has analytical advantages.

1. Introduction

Since 1978 the synthesis of "cascade molecules", known as dendrimers, is being described [1]. The research on dendrimer molecules is being characterized by an exponential growth and recently it has been coupled to nanomaterials [1–5]. Dendrimers are well-defined, highly branched macromolecules that are of intense interest as new materials in many important application areas [1,2]. Dendrimer molecules are constituted by three basic structural units [1]: (i) a multifunctional core; (ii) the branches that are structured in regular layers (shells), linked in the form of segments to the core and are termed dendrons; and, (iii) the surface is constituted by terminal functional groups. This unique architecture originates "dendritic effects" resulting in many new unprecedented properties such as a relatively low viscosity and high mechanical stability [1]. Moreover, dendrimers are excellent anchor structures for nanomaterials because [3–5]: (i) due to the uniformity of dendrimers the encapsulated nanomaterials are also well-defined and of smaller size; (ii) the encapsulation stops the agglomeration of the nanomaterials; and, (iii) the dendrimer structure allows the selective access of analytes to the encapsulated nanomaterials.

Diaminobutane-based poly(propyleneimine) dendrimers (DAB) have been applied for in vitro diagnostics [6–9], in the delivery of drugs and other therapeutic agents [10], bioimaging diagnosis [11], and sensors of heavy metals and organic pollutants [7,8,12]. The encapsulation of quantum dots (QDs) nanomaterials by dendrimers resulted in fluorescent nanocomposites with improved sensing capacities [2,13–21].

QDs are semiconductor nanomaterials which have size dependent fluorescence properties due to quantum confinement processes, i.e. the size of the nanocrystals is smaller than the Bohr exciton radius [22,23]. QDs belong to a new generation of fluorescent nanomaterials that are the basis of new improved analytical methodologies, chemical and biochemical sensors [22], fluorescence sensor for imaging of metal ions in living cells [23], detection of organic compounds [24], fluorescence probes for pH response [25], and fluorescence lifetime measurements [26]. Due to the particular relevance of dendrimer as a biological drug delivery agent [7] their coupling with QDs results is quite interesting as biological nanosensor.

In this paper four generations of the DAB dendrimer with thiolated surface functionalities were synthesized – S-DAB-G_x (x = 1, 2, 3 and 5). CdSe QDs were encapsulated in these four dendrimers,

* Corresponding author. Tel.: +351 220 402 569; fax: +351 220 402 659.
E-mail address: jcsilva@fc.up.pt (J.C.G. Esteves da Silva).

0039-9140/$ – see front matter © 2011 Elsevier B.V. All rights reserved.
doi:10.1016/j.talanta.2011.11.007

resulting in water soluble nanocomposites S-DAB-G_x (x = 1, 2, 3 and 5)-CdSe, and their fluorescent sensing properties towards metal ions was assessed. The creation of a thiolated surface on the dendrimer had a twofold objective: (i) increase the affinity towards QDs and participate in their stabilization in water; and, (ii) allowing the surface of the dendrimer to act as a ligand towards soft metal ions. Taking into consideration that both the dendrimer and QDs have affinity towards metal ions the global sensor response cannot be easily forecast. However, the comprehension of the fluorescent signal variation should give interesting information about the possible design strategies of future dendrimer/QDs nanocomposites sensors.

2. Experimental

2.1. Reagents

Polypropylenimine dendrimers DAB-AM-(4, 8, 16 and 64), generations 1, 2, 3 and 5, DAB-G_x (x = 1, 2, 3 and 5) – molecular structure shown in Supplementary Fig. A, cadmium chloride ($CdCl_2$, 99.9%), selenium powder (Se, 99.99%), *N*-hydroxysuccinimide (98%), 1,3-dicyclohexylcarbodiimide (99%) and 3-mercaptopropinoic acid (MPA, 99%) were purchased from Sigma-Aldrich Spain and sodium borohydride ($NaBH_4$, ≥96%) from Fluka. 3-Mercaptopropanyl-*N*-hydroxysuccinimide ester was synthesized by condensation reaction of *N*-hydroxysuccinimide and 3-mercaptopropionic acid in presence of 1,3-dicyclohexylcarbodiimide, following literature procedures [27]. All solutions were prepared with deionised water (resistivity higher than 4 MΩ cm^{-1}).

2.2. Synthesis of thiolated DAB dendrimers

All thiolated DAB dendrimers have been prepared following the same procedure. A solution of a 5% excess of 3-mercaptopropanyl-*N*-hydroxysuccinimide ester [27] was added drop wise to a stirred solution of the dendritic polyamine DAB-AM-(4, 8, 16 and 64) and triethylamine in CH_2Cl_2 under argon at room temperature. After stirring overnight, the resulting reaction mixture was washed three times with water and the organic layer dried over anhydrous $MgSO_4$ and evaporated. S-DAB-G_x (x = 1, 2, 3 and 5) are obtained as colourless waxy solids, insoluble in organic solvents and soluble in aqueous 0.1 M NaOH. Yields were from 33 to 60%. NMR spectra (data not shown) show the low-field shift of the dendrimer resonances thus confirming complete functionalization with the thiol groups.

2.3. Preparation of S-DAB-CdSe QDs nanocomposites

The synthesis of CdSe QDs was done as described previously [28]. To 50 mL of the previously synthesized CdSe QDs solution, 10 mg of the corresponding S-DAB-G_X (x = 1, 2, 3 and 5) was added and left stabilize for 72 h. The resulting green-yellowish fluorescent solution was dialyzed in cellophane membrane (using a MW CO 12,000–14,000 Dalton dialysis tube from Medicell International) for 12 h against deionized water at room temperature. The dialyzed solution was centrifuged at 13,000 rpm for 10 min to remove solid substances and the resulting solution was applied for sensing metal ions and used without modifications.

2.4. Instrumentation

Fluorescence measurements were made with Horiba Jovin Yvon Fluoromax 4 TCSPC spectrophotometer using an excitation of 408 nm and an emission range of 400–700 nm, with an integration time of 0.1 s and using slit widths of 5 nm for both, excitation and emission monochromators. Measurements were made on standard 1 cm path length quartz cuvette and at room temperature. Absorbance measurements were made in a Hewlett-Packard HP8452A diode array spectrophotometer. Transmission Electron Microscopy (TEM) was carried out with a Philips CM-200.

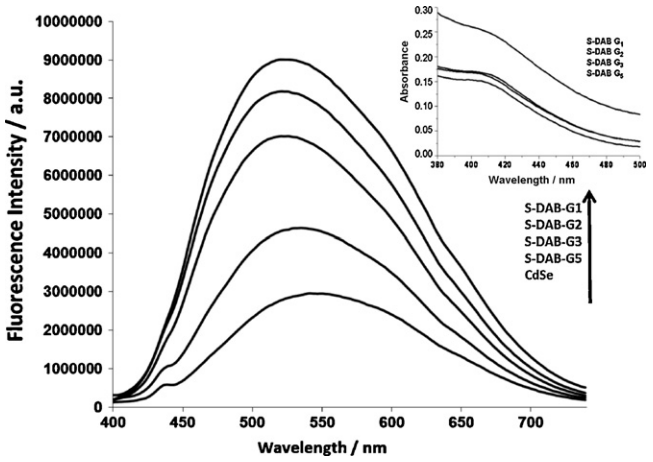

Fig. 1. Fluorescence emission spectra of the CdSe quantum dots and corresponding nanocomposites with different generations S-DAB. UV–vis spectra of the different generations of S-DAB (inserted image).

2.5. Metal ion titrations

For the metal ions analysis, 500 μL of each S-DAB-G_x (x = 1, 2, 3 and 5)-CdSe were transferred to different 5 mL calibrated flasks, with aliquots containing from 2×10^{-5} to 1×10^{-3} M and 1×10^{-5} to 1.52×10^{-4} M of Cd(II) and Pb(II), respectively. In all experiments, samples were sonicated for 5 min, left until room temperature, and then their fluorescence spectra were recorded. In order to assess the interference of some metal ions, three different aliquots of Co(II), Cu(II), Fe(II) and Zn(II) (1×10^{-4}, 5×10^{-4} and 1×10^{-3} M), were transferred into separate 5 mL calibrate flasks containing 500 μL of S-DAB-G_5-CdSe and Cd(II) or Pb(II) (1×10^{-4} M).

2.6. Fluorescence data analysis

The enhancement of the fluorescence curve by metal ions [M(II)] was described using a Henderson–Hasselbalch type equation:

$$[\mathrm{M(II)}] = K + s \log\left(\frac{I_{\max} - I}{I - I_{\min}}\right)$$

The quenching of fluorescence by metal ions [M(II)] was described using the Stern–Volmer equation:

$$\frac{I_0}{I} = 1 + K_{sv}[\mathrm{M(II)}]$$

where I_0 is the fluorescence intensity without metal ion, I is the fluorescence intensity observed in the presence of a metal ion and K_{sv} is the static Stern–Volmer constant [29].

3. Results and discussion

3.1. Characterization of S-DAB-G_x-CdSe nanocomposite

The photophysical properties of S-DAB-CdSe nanocomposites were characterized by UV–vis absorption and fluorescence spectroscopies. The UV–vis spectra (inserted in Fig. 1) are characterized by a well-defined shoulder at 408 nm. Previous studies on different generation DAB dendrimer nanocomposites with CdS QDs reported

a blue-shift of the absorption band as the generation of the dendrimer is increased due to the participation of the amine groups in the capping of the QDs [30]. This is not observed for the S-DAB-G_x dendrimers probably because now the terminal thiol groups have a major role in the QDs stabilization, the fluorescence spectra shows a light blue shift, more remarkable in low dendrimer generation, and explained by the cluster formation of the systems [31].

The fluorescence emission spectra of the CdSe QDs and of the nanocomposites with the different S-DAB-G_x dendrimers generations are shown in Fig. 1. This figure clearly shows that the dendrimers provoke an increase on the fluorescence intensity of the CdSe QDs and that the smaller the dendrimer generation the higher the increase.

The geometry and size of the S-DAB-G_x dendrimers were estimated by computational calculations and are shown in Supplementary Fig. A. The estimated diameter of the four S-DAB-G_x dendrimers was: S-DAB-G_1, 2.6 nm; S-DAB-G_2, 3.7 nm; S-DAB-G_3, 4.4 nm; S-DAB-G_5, 6.6 nm. TEM images could not give particularly useful information about the morphology of the synthesized nanocomposites (Supplementary Fig. B) but the dimensions of the CdSe QDs must be smaller than 11.2 nm [32]. Assuming that the increase in photoluminescence is due to thiol binding to the QD surface, it must be that the smaller dendrimers can fit closer together, thus allowing more thiol surface interactions.

Previous works have reported an increase in photoluminescence of nanocrystals due to binding of sulfur to the QD surface. Rene-Boisneuf and Scaiano [33] showed that treating CdSe QDs with elemental sulfur leads to fluorescence enhancement and excellent stability and Nann [34] reported that CdSe@ZnS QDs show an increase in fluorescence intensity due to addition of thiolated molecules such as mercaptoethanol.

The maximum of the emission spectra of the S-DAB-G_x-CdSe nanocomposites is blue-shift when compared with the raw CdSe QDs (541 nm): S-DAB-G_5-CdSe (535 nm); S-DAB-G_3-CdSe (520 nm); S-DAB-G_2-CdSe (520 nm); S-DAB-G_1-CdSe (520 nm). The emission full width of half maximum (FWHM) is comprised for all of them between 168–171 nm, which is a relatively high value when compared with typical narrow emission bands of QDs. This result suggests that there is a high degree of size heterogeneity, probably because they are bound to different chemical environments in the S-DAB-G_X dendrimers.

3.2. Effect of metal ions on the nanocomposite fluorescence

In order to assess if the fluorescence properties of the designed S-DAB-G_X-CdSe nanocomposites were sensible to the presence of other metal ions the effect of 1×10^{-4} M aqueous solutions of the following divalent metal ions was tested: Cr(II), Fe(II), Co(II), Ni(II), Cu(II), Zn(II), Cd(II), Hg(II) and Pb(II). The nanocomposite that shows higher impact from the metal ions presence on the fluorescence intensity is S-DAB-G_5-CdSe and it is shown in Fig. 2.

The analysis of Fig. 2 shows that almost all metal ions provoke quenching and Fe(II), Zn(II) and Cd(II) provoke enhancement of the raw S-DAB-G_5-CdSe fluorescence. Moreover, Pb(II) ions provokes the highest quenching and Cd(II) the highest enhancement which constitutes evidence that the generation five nanocomposite may constitute a useful sensor for these two ions and deserve further investigation.

The fluorescence variations that are observed when metal ions are present occur only in the intensity scale and not in the wavelength emission. This result shows that there is no change of the quantum confinement of the QDs and that the corresponding band gap energy is not affected. However, the fluorescence intensity variations are due to surface effects resulting from the complexation of the metal ions by the capping ligands of the QDs. There are two possible mechanisms to explain the variation of fluorescence intensity

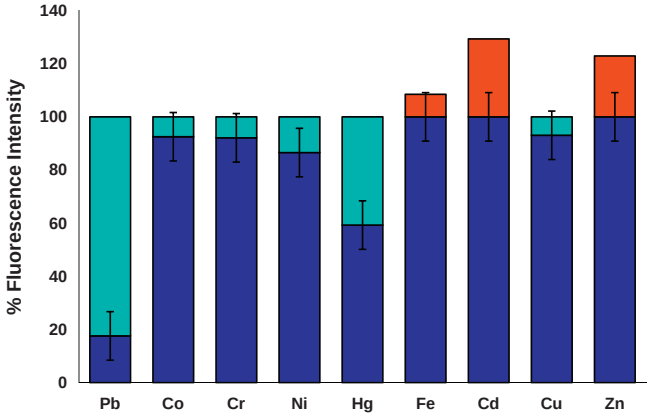

Fig. 2. Effect of the presence of metal ions on the fluorescence of S-DAB-G_5-CdSe nanocomposite.

of QDs when metal ions are present [35,20]: (i) the capping ligands bind to the metal ions present in the solution provoking its displaced from the surface of the QDs originating imperfections on the QDs surface resulting on the quenching of the fluorescence; (ii) the complexation of metal ions by surface ligands of QD provokes charge transfer processes involving the core and the surface of the QDs affecting the quantum yield. This second mechanism is the only one compatible with the fluorescence enhancement observed when Zn(II) and Cd(II) d^{10} ions (diamagnetic) are present. Fe(II) provokes a relatively small fluorescent enhancement probably because it is in a diamagnetic electronic state [36,37]. Hg(II) and Pb(II) ions are also diamagnetic but are heavy atoms ions which usually provoke quenching of the fluorescence [29]. The other studied metal ions are paramagnetic ions and provoke quenching of the fluorescence [38,39]. Taking into consideration this observation the existence of charge transfer mechanism involving the QDs valence bands and the complexed metal ions LUMO and/or HOMO is highly probable.

The structure and the functional groups (mainly those containing nitrogen and sulfur) of the dendrimer should have an important active role in the complexation of the metal ions, together with the QDs capping ligands, and must affect the complexed metal ions LUMO and/or HOMO and the charge transfer mechanism. Indeed, surrounding chemical environmental affects the conformation of the DAB dendrimers [40,41] and it should influence the emission properties of the QDs.

Taking into consideration that the fluorescence of a nanocomposite constituted by DAB and CdS QDs was highly affected by the ionic strength [2], the effect of alkaline metal ions Na^+ and K^+ was also studied. Contrary to the effect on the non thiolated DAB dendrimer nanocomposites [2] the thiolated ones suffer a relatively small quenching when relatively high ionic strengths are used (Supplementary Fig. C).

3.3. Cd(II) sensor

Fig. 3a shows the fluorescence enhancement curves of the four nanocomposites as function of the Cd(II) concentration. This figures shows that the shape of the enhancement curve is similar for the four nanocomposites but, as discussed above, the enhancement is larger for the S-DAB-G_5-CdSe nanocomposite, with a seven times intensity increase. Fig. 3b shows a hypothesis for the enhancement profiles linearization based on a Henderson–Hasselbalch type equation presented in Section 2.6.

The analysis of Fig. 3 shows that a linear trend is observed in the Cd(II) concentration range between 3 and 40 ppb (about 0.05 and 0.7×10^{-6} M). The linearization equation is (standard

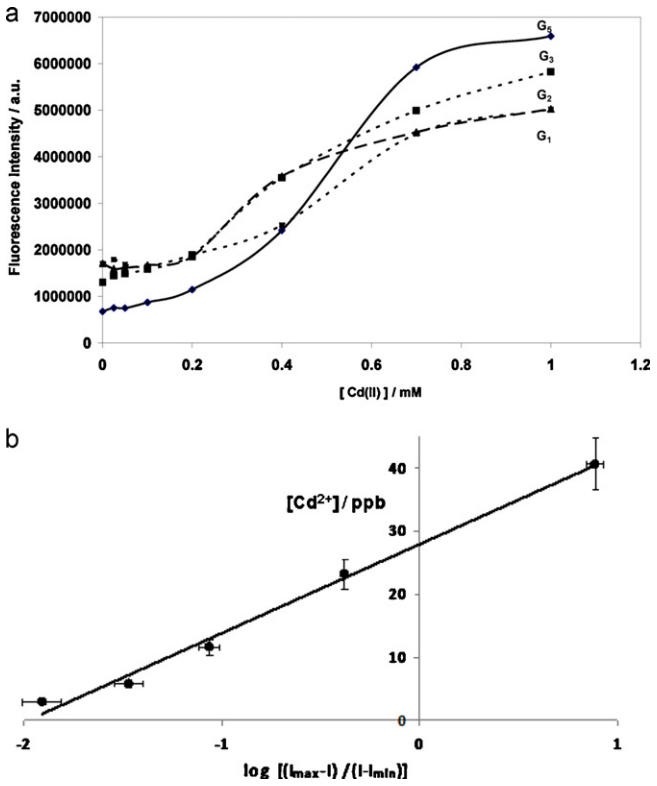

Fig. 3. The effect of Cd(II) on the fluorescence intensity of the different generation S-DAB-G_x-CdSe nanocomposites (a) and linearization of the trend corresponding to the S-DAB-G_5-CdSe nanocomposite.

deviation under parenthesis): [Cd(II)/ppb] = 27.9(0.9) + 14.0(0.7) $\log[(I_{max} - I)/(I - I_{min})]$ (correlation coefficient >0.99; $n = 5$). This shows that the fluorescence enhancement provoked by Cd(II) ions can be successful linearized and that the synthesized nanocomposites sensor respond to that ion for concentration higher than 0.05×10^{-6} M and up to 0.7×10^{-6} M.

Table 1
Stern–Volmer parameters for the quenching of different generation S-DAB dendrimer CdSe QDs nanocomposites by Pb(II) ions (8 points in the concentration range between 1×10^{-5} and 1.52×10^{-4} M).[a]

DAB-G_x-Dendrimer	K_{sv} (M^{-1})	Intercept	R
S-DAB G_1	$7.6\,(4) \times 10^3$	1.02 (3)	0.994
S-DAB G_2	$7.2\,(3) \times 10^3$	1.01 (2)	0.996
S-DAB G_3	$12.1\,(1) \times 10^3$	0.84 (2)	0.977
S-DAB G_5	$46.1\,(1) \times 10^3$	0.67 (1)	0.995

[a] Average and standard deviation (under parenthesis and referring to the last significant digit) of three independent experiences. R – Correlation coefficient.

3.4. Pb(II) sensor

Fig. 4 shows the fluorescence emission spectra of S-DAB-G_5-CdSe as function of the Pb(II) concentration. This figures clearly shows the quenching effect of the Pb(II) ion, as discussed above. The inserted figure on Fig. 4, represents the corresponding Stern–Volmer plot. In Table 1 are presented the results of the linear fit of the quenching profiles obtained with the four nanocomposites for Pb(II) ion are presented.

The analysis of Table 1 confirms the above discussion about the higher affinity of the generation five nanocomposite towards Pb(II) because it shows the highest Stern–Volmer constant (K_{sv} – standard deviation under parentheses): (generation 1) $7.6(0.4) \times 10^3\ M^{-1}$; (generation 2) $7.2(0.3) \times 10^3\ M^{-1}$; (generation 3) $12.1(0.1) \times 10^3\ M^{-1}$; (generation 5) $46.1(0.1) \times 10^3\ M^{-1}$. The four Stern–Volmer plots show a linear trend but, as the dendrimer generation increases, an upward curvature becomes detectable which provokes a deviation for the expected intercept for the nanocomposites with generation three and five DAB dendrimers. This type of deviation of the Stern–Volmer model is usually attributed to the simultaneous existence of both static and dynamic quenching [29]. However, in this case, this justification could be over simplistic and other more complex effects resulting from dendrimer conformation modifications could be occurring.

Nevertheless, although a slight upward curvature is observed in the Stern–Volmer plot when relatively high concentrations are analysed within the concentration range up to 0.1 mM the following linear equation is observed (standard deviation under parenthesis):

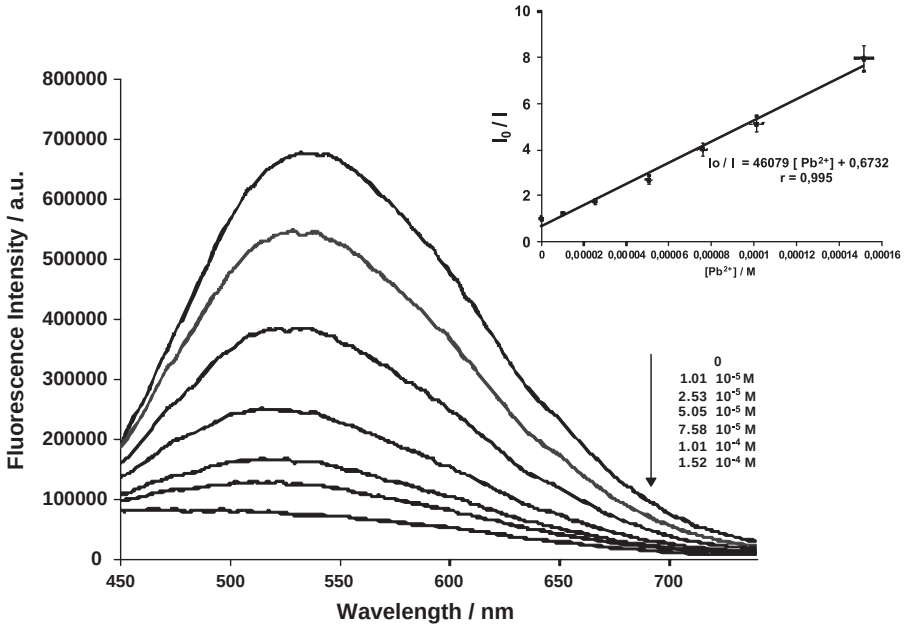

Fig. 4. The effect of Pb(II) in the emission fluorescence spectra of S-DAB-G_5-CdSe and Stern–Volmer plot of the corresponding quenching (inserted figure).

Table 2
Tolerance ratio of divalent metal ions in the fluorescence measurements of Cd(II) and Pb(II) by S-DAB-G_5-CdSe.

	S-DAB-G_5		
	Cd^{2+}/M^{2+}	Pb^{2+}/M^{2+}	Ratio
Co^{2+}	0.97	–	1:1
	0.90	–	1:5
	0.82	–	1:10
Cr^{2+}	–	0.71	1:1
	–	0.56	1:5
	–	0.24	1:10
Cu^{2+}	0.97	–	1:1
	0.92	–	1:5
	0.90	–	1:10
Fe^{2+}	0.82	0.31	1:1
	0.23	0.33	1:5
	0.04	0.10	1:10
Hg^{2+}	–	0.51	1:1
	–	0.07	1:5
	–	0.04	1:10
Zn^{2+}	1.22	–	1:1
	3.76	–	1:5
	4.33	–	1:10

$I_0/I = 0.8\,(0.1) + 42 \times 10^3\,(2 \times 10^3)\,[\mathrm{Pb(II)/M}]$ (correlation coefficient >0.99; 6 points). The linear dynamic range was established between 0.01 and 0.15 mM. The limit of detection (as $3 \times \mathrm{SD/m}$) = 6×10^{-5} M. The measurement precision was 1% (relative standard deviation).

The quenching provoked by Pb(II) in S-DAB-G_5-CdSe ($K_{SV} = 42 \times 10^3\ \mathrm{M}^{-1}$) is similar to that provoked in DAB-G_5-CdS ($K_{SV} = 22 \times 10^3\ \mathrm{M}^{-1}$) [2]. However, for the case of the Hg(II) and Cu(II) ions the S-DAB-G_5-CdSe nanocomposite has a relatively smaller affinity than DAB-G_5-CdS.

3.5. Analysis of the interferents

In order to assess the selectivity of the sensor response to Cd(II) or Pb(II) when other metal ions are present, an interference investigation was performed using solutions containing 1×10^{-4} M of the two metal ions. Table 2 shows the results obtained using the method of tolerance ratios. The analysis of this Table shows that the sensor has selectivity limitations because when Fe(II) and Hg(II) ions are equimolar quantities to Cd(II) or Pb(II) a marked interference is observed in the sensor response.

4. Conclusions

By using a new designed different generation DAB dendrimers with thiolated surface functionalities encapsulating CdSe quantum dots a new fluorescent sensor with relatively high affinity towards soft metal ions was obtained. Diamagnetic metal ions provoked an enhancement of the fluorescence and paramagnetic metal ions provoked quenching of the fluorescence. Cd(II) ion, in the submicromolar concentration range, provokes the highest fluorescence enhancement and Pb(II) ion, in the submilimolar concentration range, provokes the highest quenching. Also, taking into consideration that the DAB dendrimers are biocompatible and membrane permeable the newly developed nanosensor has potential for bioanalytical soft metal detection and quantification.

Acknowledgements

The authors would like to thank the Fundação para a Ciência e Tecnologia (Lisboa, Portugal) under the frame of the Ciência 2007 and 2008 programs and Spanish Ministerio de Ciencia e Innovación (Project CTQ2009-12332-C02-01) are acknowledged. Financial support from Fundação para a Ciência e a Tecnologia (FCT, Lisbon) (Programa Operacional Temático Factores de Competitividade (COMPETE) e comparticipado pelo Fundo Comunitário Europeu FEDER) (Project PTDC/QUI/71001/2006) is acknowledged.

Appendix A. Supplementary data

Supplementary data associated with this article can be found, in the online version, at doi:10.1016/j.talanta.2011.11.007.

References

[1] F. Vogtle, G. Richardt, N. Werner, Dendrimer Chemistry. Concepts, Syntheses, Properties, Applications, Wiley-VCH, Weinheim, 2009.
[2] B.B. Campos, M. Algarra, B. Alonso, C.M. Casado, J.C.G. Esteves da Silva, Analyst 134 (2009) 2447.
[3] M. Frasconi, C. Tortolini, F. Botre, F. Mazzei, Anal. Chem. 82 (2010) 7335.
[4] S. Guo, E. Wang, Anal. Chim. Acta 598 (2007) 181.
[5] J.M. Liu, Z.B. Liu, Q.M. Lua, F.M. Li, S.R. Hua, G.H. Zhu, X.M. Huang, Z.M. Li, X.M. Shi, Anal. Chim. Acta 598 (2007) 205.
[6] A.G. Schatzlein, B.H. Zinselmeyer, A. Elouzi, C. Dufes, Y.T.A. Chim, C.J. Roberts, M.C. Davies, A. Munro, A.I. Gray, I.F. Uchegbu, J. Control. Release 101 (2005) 247.
[7] W.E. Bawarski, E. Chidlowsky, D.J. Bharali, S.A. Mousa, Nanomed. Nanotechnol. Biol. Med. 4 (2008) 273.
[8] A.F.E. Hezinger, J. Tessmar, A. Gopferich, Eur. J. Pharm. Biopharm. 68 (2008) 138.
[9] T. Dutta, M. Garg, N.K. Jain, Eur. J. Pharm. Sci. 34 (2008) 181.
[10] H.L. Crampton, E.E. Simanek, Polym. Int. 56 (2007) 489.
[11] R.W.J. Scott, O.M. Wilson, R.M. Crooks, J. Phys. Chem. B 109 (2005) 692.
[12] N. Lubick, Environ. Sci. Technol. 43 (2009) 1247.
[13] B.K. Sooklal, L.H. Hanus, C.J. Murphy, Adv. Mater. 10 (1998) 1083.
[14] B.I. Lemon, R.M. Crooks, J. Am. Chem. Soc. 122 (2000) 12886.
[15] R.C. Hedden, B.J. Bauer, A.P. Smith, F. Gröhn, E. Amis, Polymer 43 (2002) 5473.
[16] B. Huang, D.A. Tomalia, J. Luminesc. 111 (2005) 215.
[17] A.C. Wisher, I. Bronstein, V. Chechik, Chem. Commun. 15 (2006) 1637.
[18] S.K. Gayen, M. Brito, B.B. Das, G. Comanescu, X.C. Liang, M. Alrubaiee, R. Alfano, C. González, A.H. Byro, D.L. Bauer, V. Balogh-Nair, J. Opt. Soc. Am. B 24 (2007) 3064.
[19] J. Ling, R.M. Cong, Acta Chim. Sinica 18 (2008) 2070.
[20] B.B. Campos, M. Algarra, J.C.G. Esteves da Silva, J. Fluoresc. 20 (2010) 143.
[21] J.G.G. Esteves da Silva, M. Algarra, B.B. Campos, in: B. Reddy (Ed.), Synthesis and Analytical Applications of Quantum Dots Coated with Different Generations of DAB Dendrimers, Advances in Nanocomposites - Synthesis, Characterization and Industrial Applications, IN-TECH, Rijeka, Croatia, 2011.
[22] M.F. Frasco, N. Chaniotakis, Sensors 9 (2009) 7266.
[23] A.M. Smith, N. Shuming, Acc. Chem. Res. 43 (2010) 190.
[24] A.C. Vinayaka, S. Basheer, M.S. Thakur, Biosens. Bioelectron. 24 (2009) 1615.
[25] H. Kobayashi, M. Ogawa, R. Alford, P.L. Choyke, Y. Urano, Chem. Rev. 110 (2010) 2620.
[26] M.Y. Brezin, S. Achilefu, Chem. Rev. 110 (2010) 2641.
[27] S. Connolly, S.N. Rao, D. Fitzmaurice, J. Phys. Chem. B 104 (2000) 4765.
[28] M. Algarra, B.B. Campos, J.C.G. Esteves da Silva, Talanta 83 (2010) 1335.
[29] J.R. Lackowiz, Principles of Fluorescence Spectroscopy, 2nd ed., Springer, New York, 1999.
[30] S.K. Gayen, M. Brito, B.B. Das, G. Comanescu, X.C. Liang, M. Alrubaiee, R.R. Alfano, C. González, A.H. Byro, D.L.V. Bauer, V. Balogh-Nair, J. Opt. Soc. Am. B 24 (2007) 3064.
[31] B. Pan, F. Gao, L. Ao, H. Tian, R. He, D. Cui, Coll. Surf. A: Physicochem. Eng. Aspects 259 (2005) 89.
[32] T. Kippeny, L.A. Swafford, S.J. Rosenthal, J. Chem. Ed. 79 (2002) 1094.
[33] L. Rene-Boisneuf, J.C. Scaiano, Chem. Mater. 20 (2008) 6638.
[34] T. Nann, Chem. Commun. (2005) 1735.
[35] H. Gonçalves, C. Mendonça, J.C.G. Esteves da Silva, J. Fluoresc. 19 (2009) 141.
[36] C.S.P.C.O. Silva, J.C.G. Esteves da Silva, A.A.S.C. Machado, Appl. Spectrosc. 48 (1994) 363.
[37] J.C.G. Esteves da Silva, A.A.S.C. Machado, Appl. Spectrosc. 50 (1996) 436.
[38] J.C.G. Esteves da Silva, A.A.S.C. Machado, C.J.S. Oliveira, Anal. Chim. Acta 349 (1997) 23.
[39] J.C.G. Esteves da Silva, A.A.S.C. Machado, C.J.S. Oliveira, M.S.S.D.S. Pinto, Talanta 45 (1998) 1155.
[40] P. Welch, M. Muthukumar, Macromolecules 31 (1998) 5892.
[41] A. Ramzi, R. Scherrenberg, J. Joosten, P. Lemstra, K. Mortensen, Macromolecules 35 (2002) 827.